

Pu-erh tea extract ameliorates high-fat diet-induced nonalcoholic steatohepatitis and insulin resistance by modulating hepatic IL-6/STAT3 signaling in mice

Xianbin Cai^{1,2,4} · Chongye Fang^{2,3} · Shuhei Hayashi^{2,4} · Shumei Hao⁵ · Mingming Zhao⁶ · Hiroko Tsutsui^{2,4} · Shuhei Nishiguchi¹ · Jun Sheng³

Received: 4 June 2015 / Accepted: 27 November 2015
© Japanese Society of Gastroenterology 2016

Abstract

Background Pu-erh tea, made from the leaves of *Camellia sinensis*, possesses activities beneficial for human health, including anti-inflammatory, anti-oxidant, and anti-obesity properties.

Objective We investigated the effects of a pu-erh tea extract (PTE) on nonalcoholic steatohepatitis (NASH) and the molecular mechanisms underlying such effects.

Methods Eight-week-old male C57BL/6J mice were fed a normal chow diet or high-fat diet (HFD) for 17 weeks, during which PTE was simultaneously administered in drinking water. Body weight, hepatic inflammation, steatosis, insulin sensitivity, expression of lipogenesis- and gluconeogenesis-associated genes, and signal transducer and activator of transcription (STAT)-3 phosphorylation were examined. The anti-steatotic effects of PTE and/or interleukin (IL)-6 were evaluated in HepG2 cells. The lipid accumulation, STAT3 phosphorylation, and expression of lipid metabolism-related genes were analyzed.

Results PTE inhibited HFD-induced obesity and significantly attenuated HFD-induced hepatic steatosis and liver inflammation, and prevented against liver injury. PTE treatment improved glucose tolerance and insulin sensitivity in HFD-fed mice. Moreover, PTE treatment maintained the intact insulin signal and significantly decreased expression of gluconeogenesis-related genes in the livers of HFD-fed mice. PTE treatment strikingly enhanced STAT3 phosphorylation in the livers of HFD-fed mice. Consistent with this increase in STAT3 phosphorylation, pre-treatment of HepG2 cells with PTE enhanced IL-6-induced STAT3 phosphorylation and attenuated oleic acid-induced steatosis in a STAT3-dependent manner. In contrast, PTE inhibited IL-6-induced STAT3 phosphorylation in macrophages.

Conclusions PTE ameliorates hepatic lipid metabolism, inflammation, and insulin resistance in mice with HFD-induced NASH, presumably by modulating hepatic IL-6/STAT3 signaling.

Xianbin Cai, Chongye Fang and Shuhei Hayashi have been contributed equally to this work.

Electronic supplementary material The online version of this article (doi:10.1007/s00535-015-1154-0) contains supplementary material, which is available to authorized users.

✉ Shuhei Nishiguchi
nishiguc@hyo-med.ac.jp

✉ Jun Sheng
shengjunpuer@yahoo.com.cn

- ¹ Division of Hepatobiliary and Pancreatic Diseases, Hyogo College of Medicine, 1-1 Mukogawa-cho, Nishinomiya, Hyogo 663-8501, Japan
- ² Department of Pu-erh Tea and Medical Science, Hyogo College of Medicine, 1-1 Mukogawa-cho, Nishinomiya, Hyogo 663-8501, Japan
- ³ Key Laboratory of Pu-erh Tea Science, The Ministry of Education, Yunnan Agricultural University, Kunming 650201, People's Republic of China
- ⁴ Department of Microbiology, Hyogo College of Medicine, 1-1 Mukogawa-cho, Nishinomiya, Hyogo 663-8501, Japan
- ⁵ Yunnan University, Kunming 650091, People's Republic of China
- ⁶ Center for iPS Cell Research and Application (CiRA), Kyoto University, Sakyo-ku, Kyoto 606-8502, Japan

Keywords PTE · STAT3 · NASH · Insulin resistance

Abbreviations

PTE	Pu-erh tea extract
NAFLD	Nonalcoholic fatty liver disease
NASH	Nonalcoholic steatohepatitis
ND	Normal chow diet
HFD	High-fat diet
STAT3	Signal transducer and activator of transcription 3
p-STAT3	Phosphorylated STAT3

Introduction

Nonalcoholic fatty liver disease (NAFLD), characterized by ectopic accumulation of triglycerides in the liver, is one of the most prevalent diseases of the liver. Patients with NAFLD often progress to the severe disease designated as nonalcoholic steatohepatitis (NASH), which is defined by additional liver injury and inflammation. A subset of patients with NASH develops cirrhosis and hepatocellular carcinoma [1–3]. NAFLD/NASH is closely associated with obesity and insulin resistance [1, 3, 4]. The prevalence of NAFLD/NASH-related liver disease is rising worldwide, including Asia [5, 6]. However, the mechanisms underlying the progression of NASH remain largely unclear. Moreover, there are no validated treatments for NASH other than managing obesity and associated metabolic abnormalities through lifestyle modification [7].

The “two-hits” model of NASH pathogenesis was proposed by Day et al. [8]. According to the “two-hit” hypothesis, insulin resistance and ectopic intracellular lipid accumulation in hepatocytes initiate NAFLD, while subsequent inflammation and lipid oxidation lead to liver injury. Cytokines and chemokines are involved in the activation of Kupffer cells and tissue macrophages in the liver, as well as in the recruitment of other inflammatory cells, promoting hepatic inflammation. Pro-inflammatory cytokines/chemokines, such as tumor necrosis factor- α (TNF- α), interleukin (IL-6), monocyte chemoattractant protein-1 (MCP-1), and IL-1 β , play a critical role in the progression of NAFLD to more advanced stages of liver damage [9]. Insulin resistance and glucose metabolism disorder are found in most NAFLD/NASH patients [1, 3, 4]. Ad libitum access to a high-fat diet (HFD) in mice causes obesity, insulin resistance, hepatic steatosis, hypercholesterolemia, and dyslipidemia [10]. It is important to develop an ideal treatment for NAFLD/NASH that can attenuate hepatic steatosis and inflammation while improving insulin resistance.

Pu-erh tea, a fermented dark tea made from the leaves of *Camellia sinensis*, is known for its multiple biological effects, which include hypolipidemic, hypocholesterolemic,

antiobesity, antidiabetic, antioxidant, and antibacterial actions [11, 12]. Accumulating lines of evidence demonstrate that pu-erh tea extract (PTE) improves insulin resistance and ameliorates NAFLD in mouse models of obesity and diabetes, including *ob/ob* and *db/db* mice, which are leptin- and leptin receptor-deficient, respectively [13, 14]. However, the mechanism underlying prevention of NAFLD by PTE remains to be elucidated. The signal transducer and activator of transcription 3 (STAT3) is regarded as a potent endogenous regulator of NASH [15]. Thus, we hypothesized that PTE might rescue mice from NASH by enhancing IL-6/STAT3 signaling. The present study was designed to investigate this possibility using a NASH model induced by high-fat diet in normal wild-type mice.

Materials and methods

Reagents and antibodies

PTE was generously supplied by the China Academy of Pu-erh Tea Research [16]. PTE was prepared in distilled water, and the pH was adjusted to 7.4. Recombinant human interleukin (IL)-6 was purchased from PeproTech (Rocky Hill, NJ, USA) and dissolved in 1 % bovine serum albumin (BSA) in phosphate-buffered saline (PBS). The STAT3 inhibitor stattic [17] was purchased from EMD Millipore (Darmstadt, Germany). Oleic acid-albumin (OA) and palmitate (PA) were purchased from Sigma (Darmstadt, Germany). Anti-STAT3, anti-phosphorylated (p-STAT3), anti-AMPK (5' AMP-activated protein kinase), anti-phosphorylation of AMPK (anti-p-AMPK), anti-AKT (protein kinase B), anti-phosphorylation of AKT (anti-p-AKT), anti-JNK (c-Jun N-terminal kinase), anti-phosphorylation of JNK (anti-p-JNK), and anti-STAT5 antibody were purchased from Cell Signaling Technology (Beverly, MA, USA). Anti-CD36 antibody was purchased from Abcam (Cambridge, UK). Anti-sterol regulatory element-binding protein-1c (SREBP-1c), anti- β -actin, and horseradish peroxidase-conjugated secondary antibodies were purchased from Santa Cruz Biotechnology (Santa Cruz, CA, USA), Sigma-Aldrich (St. Louis, MO, USA), and Thermo Scientific (Waltham, MA, USA), respectively.

Animals and treatments

Eight-week-old male C57BL/6J mice were purchased from CLEA Japan, Inc. (Tokyo, Japan). Mice had ad libitum access to water and food and were kept under a 12-h light–dark cycle for 1 week to adapt to the housing environment. Twenty mice were randomly divided into four groups and fed either a normal chow diet (ND) or a high-fat diet (HFD, HFD-60; Oriental Yeast Co. Ltd., Tokyo, Japan) with or without PTE in drinking water (5 mg/mL) for 17 weeks.

The PTE was replaced 1–2 times per week to maintain freshness. Food intake and body weight were monitored weekly throughout the experiments. Mice were bred in specific pathogen-free facilities at the Hyogo College of Medicine. All experimental procedures were performed in accordance with the guidelines of the Hyogo College of Medicine Committee for Care and Use of Laboratory Animals and were approved by the Animal Experiments Ethics Committee of the Hyogo College of Medicine. At the end of the experiment, mice were euthanized by isoflurane inhalation. The plasma and liver were collected and stored at -80°C .

Intraperitoneal glucose tolerance tests (IPGTTs) and intraperitoneal insulin tolerance tests (IPITTs)

Mice were injected intraperitoneally with glucose (1 g/kg body weight, after a 16-h fast) or insulin (Novolin R, Novo Nordisk, Bagsværd, Denmark; 0.5–1 U/kg body weight, no fasting) for IPGTTs and IPITTs, respectively. Blood was sampled prior to the injection and at 0, 30, 60, 90, and 120 min post-injection. Blood glucose concentrations were measured using the OneTouch UltraSmart blood glucose monitoring system (LifeScan Inc., Milpitas, CA, USA).

Cell culture and treatment

HepG2 human hepatocellular carcinoma cells (ATCC, Manassas, VA, USA) were passaged using Dulbecco's modified Eagle's medium (DMEM) containing 10 % fetal bovine serum. RAW264.7 murine macrophage (ATCC) and U937 human myeloid cells (ATCC) were grown in RPMI-1640 medium supplemented with 10 % fetal bovine serum. The assay for oleic acid (OA) induction of intracellular lipid accumulation was performed according to [18]. Briefly, 2×10^4 cells were seeded into 24-well plates 24 h prior to treatments at approximately 60 % confluence. HepG2 cells were cultured for 24 h in the presence of PTE, and the cells were treated with or without stactic (5 μM) for 1 h, followed by IL-6 and/or OA for 24 h. Cells incubated with 0.1 % BSA alone were used as controls.

RAW264.7 and U937 cells were incubated with PTE (200 $\mu\text{g}/\text{mL}$) or stactic (5 μM) for 1 h, IL-6 (2 ng/mL) was added, and the cells were subjected to an additional 15-min incubation. The cells were collected and stored at -80°C until the western blotting analysis.

Biochemical analysis of plasma samples

Plasma aspartate aminotransferase (AST), alanine aminotransferase (ALT), fasting blood sugar (FBS), free fatty acid (FFA), and total cholesterol (CHO) levels were measured (SRL, Osaka, Japan).

Evaluation of intracellular lipid accumulation and fecal lipid content

Lipid accumulation in HepG2 cells was evaluated by Oil Red O (ORO) staining and measurement of triglyceride (TG) content. Briefly, samples were fixed with 4 % paraformaldehyde and stained with ORO for 10 min, followed by counterstaining with hematoxylin for 2 min. Stained samples were examined by light microscopy. The concentrations of cellular TG and were determined using an EnzyChromTM TG assay kit and normalized to the total protein concentration according to the protocol provided by the manufacturer (Bioassay Systems, Hayward, CA, USA) [19]. Fecal lipids were extracted using the method of Folch et al. [20] with some modifications. Briefly, for the analysis of fecal lipids, feces were collected from mice housed individually in metabolic cages for a 24-h period. Aliquots of feces (100 mg) were cleaned, dried for 1 h at 70°C , disrupted with 0.5 mL of chloroform–methanol (2:1) using a Micro Smash MS-100 (Tomy Seiko Co., Tokyo, Japan), and centrifuged until a three-phase separation was observed. The middle chloroform phase was removed and transferred to a new tube, after which the fecal lipid extracts were assayed with the enzyme assay kits Wako TG-E (Wako, Osaka, Japan).

Histological and immunohistological analyses

For mouse liver histological studies, livers were perfused through a portal vein with PBS and liver specimens were rapidly sampled, fixed in 10 % neutral buffered formalin phosphate (Fisher Scientific), and embedded in paraffin. Tissue sections were prepared and stained with hematoxylin and eosin (HE). For ORO staining, liver tissues were fresh-frozen in liquid nitrogen with OCT compound (Sakura Finetek Inc., Torrance, CA, USA) and stored at -80°C . HE-stained sections were scored in terms of the NAFLD activity [21]. Hepatic steatosis was quantified via image analysis by dividing ORO-positive area by the total cellular area in each image using ImageJ software (National Institutes of Health, Bethesda, MD, USA) [22]. For immunostaining of p-STAT3, liver tissue sections were incubated overnight with anti-p-STAT3 (pTyr705) antibodies (1:5000), followed by treatment with the rabbit Vectastatin Elite ABC kit (Vector Laboratories, Burlingame, CA, USA). Antigen–antibody complexes were visualized using a DAB Substrate Kit (Vector Laboratories) [23, 24].

Western blot analysis

Western blot analysis was performed as described elsewhere [16]. Cultured cells were lysed in RIPA buffer

(Thermo Scientific, Waltham, MA, USA). Murine liver specimens were added to T-PER (Pierce, Rockford, IL, USA), and then homogenized using a Micro Smash MS-100. The proteins were separated by SDS-PAGE and transferred to Immun-Blot PVDF membranes (Bio-Rad, Hercules, CA, USA). The membranes were washed, blocked, and incubated with the primary antibody and then with an appropriate horseradish peroxidase-conjugated secondary antibody. The signal was detected with SuperSignal Dura Substrate (Pierce, Rockford, IL, USA). The images were scanned and the relative density of immunoreactive bands was determined using the Quantity One software.

Quantitative reverse transcription PCR (qRT-PCR)

Total RNA was extracted using the RNeasy Mini Kit (Qiagen, Hilden, Germany). cDNA was synthesized using the PrimeScript RT Reagent Kit (TaKaRa Bio, Otsu, Japan). qRT-PCR was performed with Taqman Universal PCR Master Mix (Applied Biosystems, Foster City, CA, USA) to measure *PPAR α* and with SYBR Premix Ex Taq II (TaKaRa Bio, Otsu, Japan) to quantify mRNA expression levels of the other molecules (summarized in Supplementary Table 1) in a Thermal Cycler Dice[®] Real Time System TP800 (TaKaRa Bio, Otsu, Japan). All the primer/probe sets were purchased from Applied Biosystems (Foster City, CA, USA). Relative expression of target gene mRNA was normalized to the amount of *18s* rRNA.

Statistical analysis

All data are expressed as the mean \pm SD of the results for the samples in each experimental group or triplicate samples. Each experimental group consisted of five mice. Differences between groups were evaluated statistically using Student's *t* test. *P* values of less than 0.05 were considered significant. Each experiment was repeated separately at least three times with similar results. Representative data are shown.

Results

PTE reduced HFD-induced weight gain, hyperlipidemia, and steatohepatitis in mice

Mice fed HFD without PTE exhibited rapid body weight gain during the first 2 weeks of the feeding period in comparison with the ND-fed mice ($P < 0.05$) (Fig. 1a). However, HFD-fed mice treated with PTE did not show a significant difference in body weight in comparison with the ND-fed mice until 12 weeks into the study (Fig. 1a).

We analyzed the effect of PTE on daily food intake and total fecal TG content, which was calculated by multiplying daily fecal mass by the TG concentration. No differences were observed between the control and PTE-treated mice in total fecal TG content (Fig. 1b, c). In HFD-fed mice with PTE, plasma fasting blood glucose (FBS), FFA, and CHO levels were significantly decreased in comparison with mice fed the HFD without PTE ($P < 0.05$; Fig. 1d–f). Hepatic steatosis is associated with decreased liver function, while elevated plasma activity of ALT and/or AST is a marker of hepatocellular damage. We detected lower levels of ALT and AST in the plasma of mice given HFD with PTE than in that of mice fed HFD without PTE (Fig. 1g, h).

Treatment with PTE significantly improved markers of HFD-induced metabolic disorders. We found increased liver weight in the mice fed HFD without PTE, but not in mice fed HFD with PTE, which suggested that HFD induced hepatic lipid accumulation that was prevented by PTE, indicating a protective effect against hepatic steatosis (Fig. 1i). To investigate whether PTE protected against NAFLD, we performed histological analyses. In ND-fed mice, HE and ORO staining revealed normal hepatic architecture within the clear hepatic lobules without any lipid droplets. In contrast, the livers of HFD-fed mice possessed many large and small lipid droplets and inflammatory cell infiltration (Fig. 1j–l). Notably, treatment with PTE significantly improved markers of HFD-induced metabolic disorders (Fig. 1i–l). These results strongly indicated that PTE protected against HFD-induced systemic and liver alterations without affecting food intake and fecal lipid excretion.

PTE enhanced IL-6/STAT3 signaling in cultured hepatocytes and the mouse liver

Several articles reported that IL-6/STAT3 activation attenuated lipid accumulation in hepatocytes [15, 25, 26]. To investigate whether PTE affected STAT3 activation, we examined STAT3 phosphorylation levels by western blotting and immunohistological analyses in vivo. Surprisingly, PTE treatment increased the number of hepatocytes with nuclear STAT3 phosphorylation in HFD-fed and ND-fed mice (Fig. 2a, b). Because of frequent translocation of gut microbiota-derived LPS, liver immune cells (e.g., Kupffer cells) are believed to produce IL-6 under normal conditions [27, 28]. Therefore, we investigated whether PTE augmented IL-6-induced STAT3 phosphorylation in hepatocytes in vitro. In HepG2 cells, PTE enhanced STAT3 phosphorylation induced by IL-6 in a dose- and time-dependent manner (Fig. 2c, d). These results suggested that PTE enhanced IL-6/STAT3 signaling in the hepatocytes of HFD-fed mice.

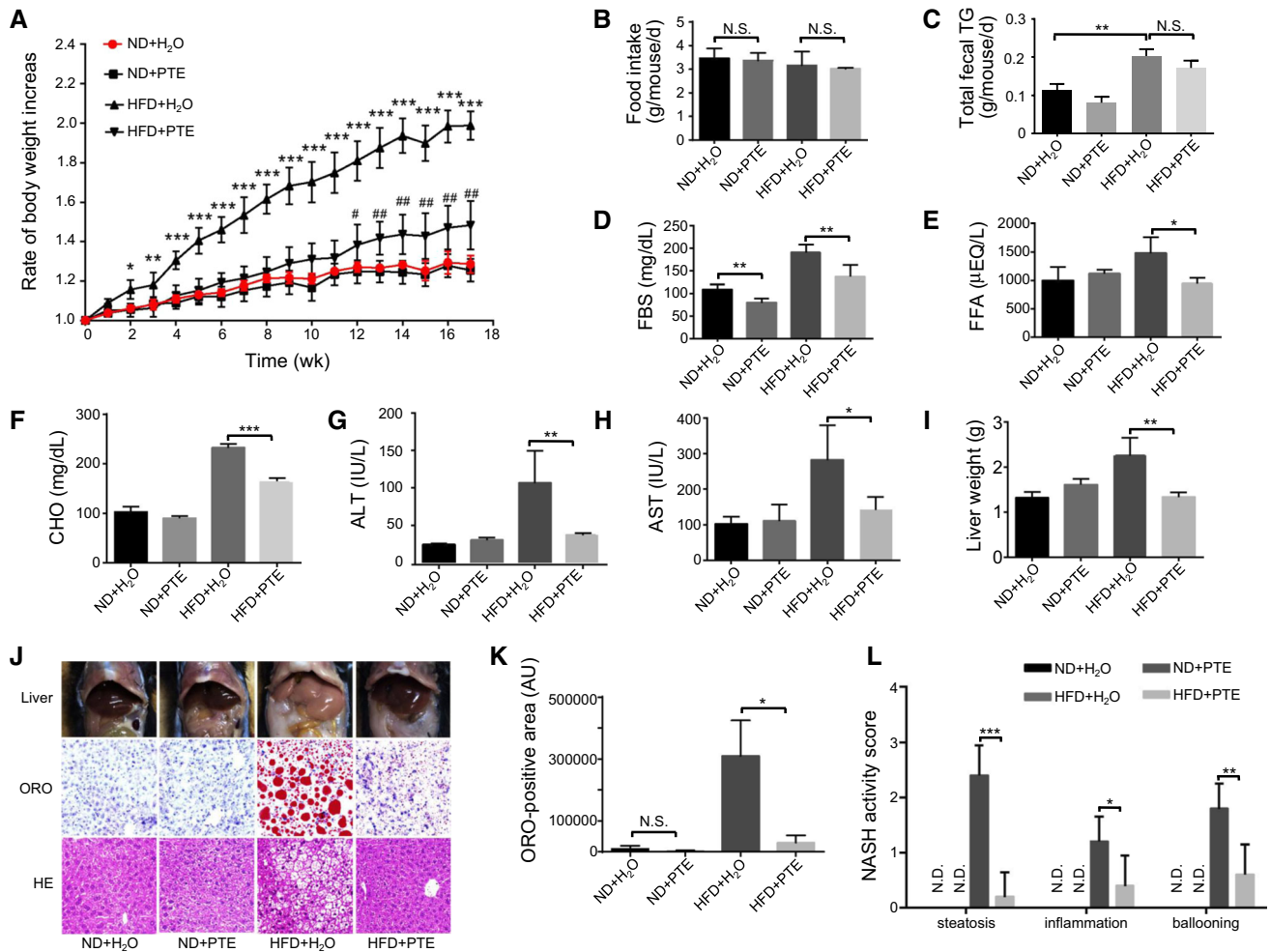


Fig. 1 PTE ameliorates HFD-induced obesity, hyperlipemia, and steatohepatitis without affecting food intake or fecal lipid excretion. C57BL/6 mice were fed ND or HFD with PTE for 17 weeks. Blood samples and liver specimens were collected promptly after the animals were euthanized. **a** Body weight was measured weekly. The ratio of the measured body weight to the body weight at day 0 was calculated. Food intake (**b**) and total fecal TG (**c**) were expressed as the mass of the food consumed by each mouse and the TG levels in its feces, respectively, on each day of the experiment. Plasma levels of **d** fasting blood sugar (FBS), **e** free fatty acid (FFA), **f** cholesterol

(CHO), **g** alanine aminotransferase (ALT), and **h** aspartate aminotransferase (AST) were measured. **i** The liver was collected and weighed. **j** Representative morphology (*top panels*), ORO staining (*middle panels*), and HE staining (*bottom panels*) of liver samples from mice in the groups with different feeding conditions are shown. The original magnification was $\times 200$. The ORO-positive area (**k**) and NAFLD activity score of each mouse group (**l**) were calculated. The displayed values are mean \pm SD ($n = 5$). * $P < 0.05$, ** $P < 0.01$, *** $P < 0.001$ for HFD + H₂O versus HFD + PTE; # $P < 0.05$, ## $P < 0.01$ for HFD + PTE versus ND + H₂O

IL-6/STAT3 signaling was involved in reduction of lipid accumulation and modulation of lipogenesis-related molecule expression in the liver by PTE

PTE markedly attenuated hepatic steatosis and activated IL-6/STAT3 signaling. Therefore, we further explored the relationship between hepatic steatosis and IL-6/STAT3 signaling using an OA-induced HepG2 cell steatosis model. PTE and IL-6 each reduced OA-induced cellular lipid accumulation (Fig. 3a). Interestingly, the combination of PTE and IL-6 appeared to inhibit lipid droplet formation

more effectively than PTE or IL-6 alone (Fig. 3a). To substantiate this result further, we measured intracellular TG and found significant inhibitory effects similar to those detected by ORO staining (Fig. 3a). To evaluate the molecular mechanism underlying these effects, we analyzed the expression levels of lipogenesis-related genes. PTE and IL-6 alone suppressed SREBP-1c protein expression in HepG2 cells. Moreover, the inhibitory effect of the combination of PTE and IL-6 on SREBP-1c protein expression was more significant than the effects of either treatment alone (Fig. 3b). PTE also enhanced *PPAR α*

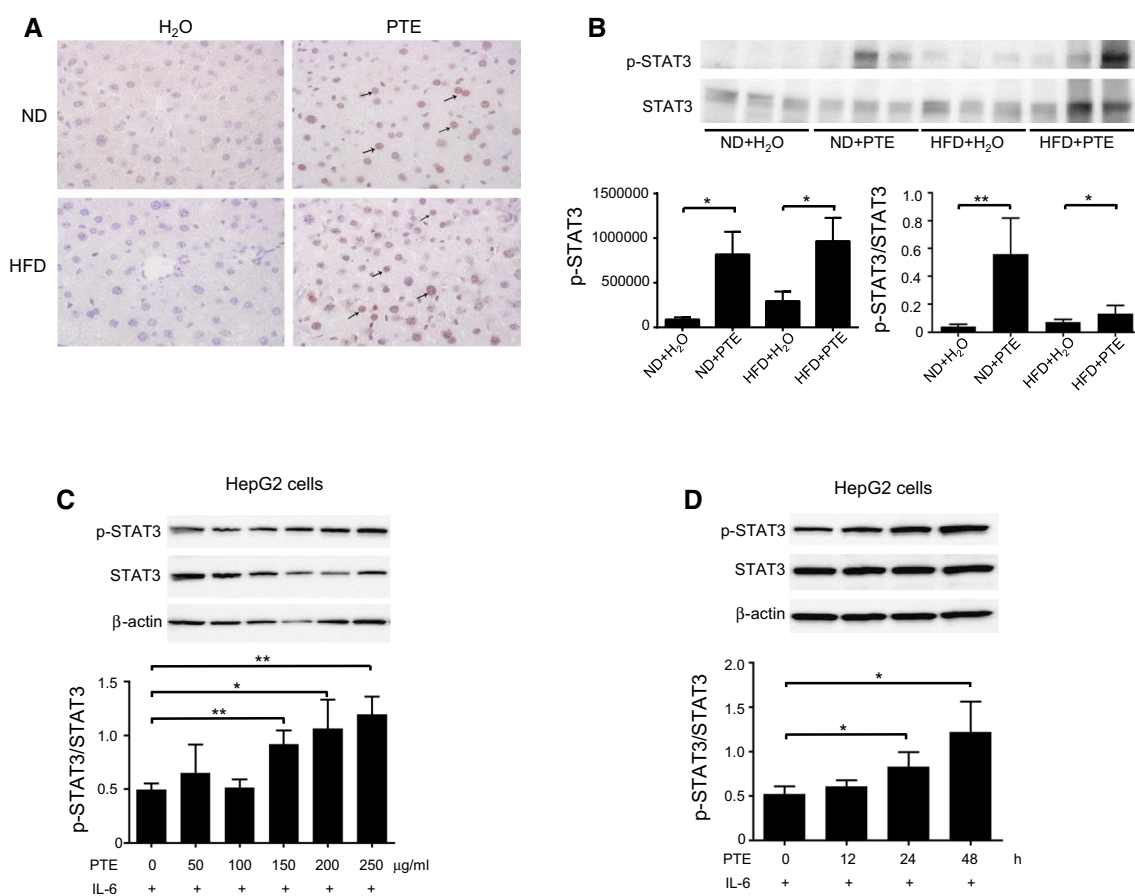


Fig. 2 PTE enhances hepatocytic STAT3 signaling in vivo and in vitro. **a** Representative immunohistochemistry for p-STAT3 in the liver samples from ND-fed or HFD-fed mice with or without PTE using anti-phospho-STAT3 (Tyr705) antibodies is shown. The *arrows* indicate the hepatocytes with p-STAT3 nuclear staining. The original magnification was $\times 200$. **b** Western blotting of liver lysates from ND-fed and HFD-fed mice with or without PTE was performed using anti-p-STAT3 (Tyr705) and anti-STAT3 antibodies. The p-STAT3 level and p-STAT3/STAT3 ratio was quantified and statistical analysis was

performed. $*P < 0.05$. HepG2 cells were incubated with different concentrations of PTE for 24 h (**c**) or with 200 $\mu\text{g}/\text{mL}$ PTE for the indicated durations (**d**), followed by the addition of IL-6 (2 ng/mL) for 15 min. Expression levels of p-STAT3, total STAT3, and β -actin were detected by western blotting. The p-STAT3/STAT3 ratio was quantified and statistical analysis was performed. The values are the mean \pm SD of three independent experiments. $*P < 0.05$, $**P < 0.01$ compared with the untreated control group

mRNA expression in HepG2 cells, while IL-6 did not (Fig. 3c). In vivo experiments revealed that PTE treatment diminished the protein levels of SREBP-1c, and down-regulated the mRNA expression levels of *Fas*, *Acc*, *Scd1*, and *Elovl6* in the livers of HFD-fed mice (Fig. 3d, e).

Because PTE reduced hepatic steatosis in parallel with enhancing of STAT3 phosphorylation, we assumed that endogenous IL-6 could prevent hepatocellular TG accumulation via STAT3 signaling and that exogenous PTE augmented this effect by enhancing STAT3 signaling. To test this possibility, we blocked STAT3 signaling with the STAT3 phosphorylation inhibitor stattic prior to treatment with IL-6 and PTE in HepG2 cells with OA-induced steatosis. Blockade of STAT3 signaling by stattic abolished the decreases in lipid accumulation, TG content, and SREBP-1c level produced by PTE and/or IL-6

(Fig. 3f, g). Since non-phosphorylated STAT5 has been reported to control steatosis via induction of CD36 expression as well [29], we investigated whether PTE and/or IL-6 treatment induced STAT5 and CD36 expressions in HepG2 cells. We found that PTE and/or IL-6 did not significantly upregulate both proteins (Supplementary Fig. 1). Furthermore, recent reports suggested that Akt, JNK, and AMPK activities are involved in the anti-steatosis effect of PTE [30, 31]. However, the PTE we used and/or IL-6 did not affect the levels of p-Akt, p-JNK, or p-AMPK in HepG2 cells (Supplementary Fig. 2). Collectively, these results demonstrate the importance of IL-6/STAT3 signaling for the regulation of lipid accumulation in HepG2 cells by PTE and suggest that the same mechanism could be involved in the beneficial effects of PTE in the livers of HFD-fed mice.

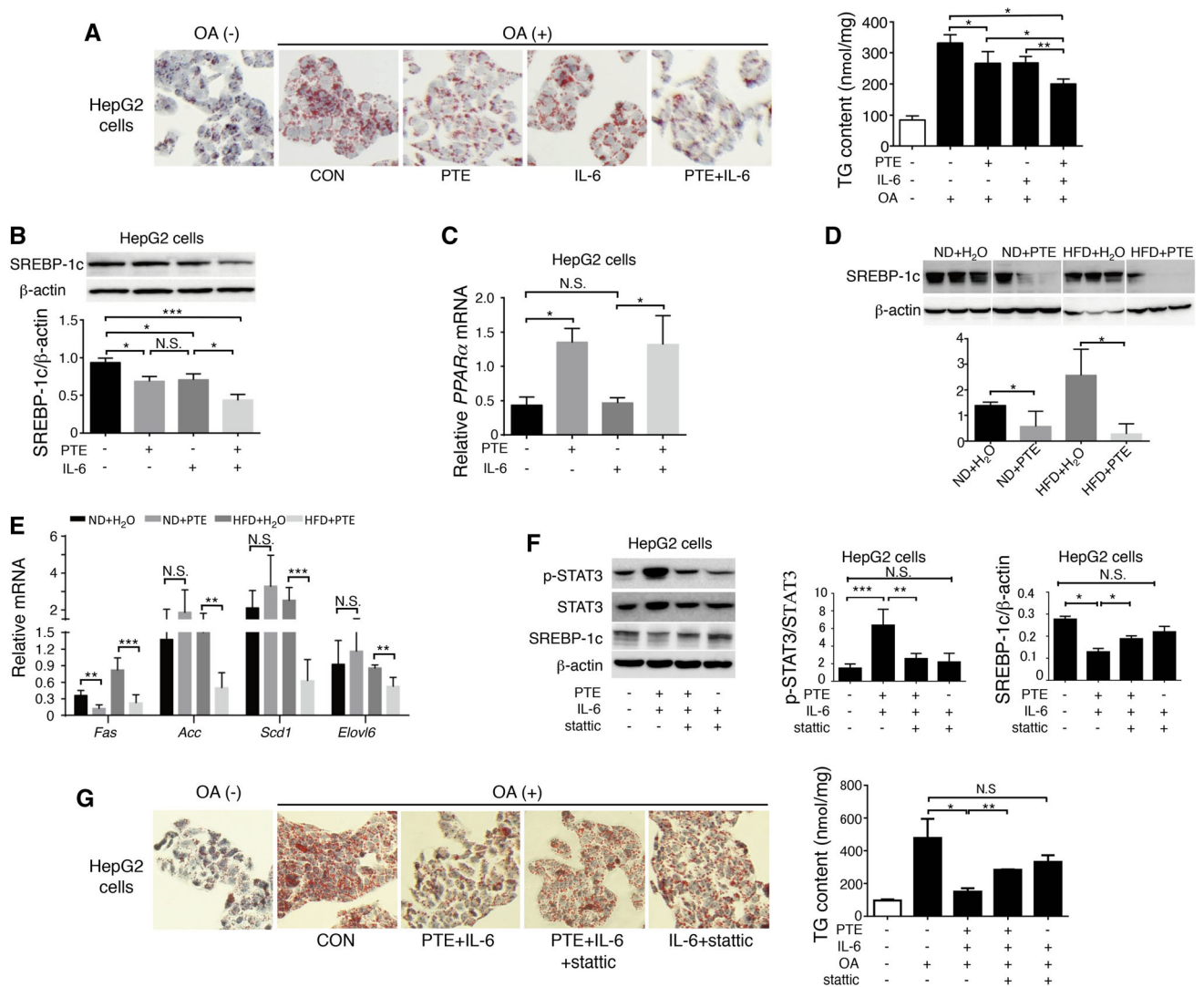


Fig. 3 PTE prevents hepatocytic lipid accumulation. **a** HepG2 cells were incubated with 200 µg/mL PTE for 24 h, followed by OA (4 µM) for 24 h in the presence or absence of IL-6 (8 ng/mL). ORO staining was performed. Intracellular TG levels were quantified. The original magnification was ×200. **b** HepG2 cells were cultured for 24 h in the presence of PTE, with or without IL-6 for 8 h. Western blotting of HepG2 cell lysates was performed using anti-SREBP-1c antibodies. The results were quantified and statistical analysis was performed. **c** Relative PPARα mRNA expression in HepG2 cells was analyzed by qRT-PCR and normalized to 18S rRNA. **d** Western blotting of liver homogenates was performed using anti-SREBP-1c antibodies. The western blot results were quantified and statistical analysis was performed. **e** Liver lysates and total RNA were prepared

from ND-fed or HFD-fed mice with or without PTE. Relative mRNA expression of lipogenesis-related genes *Fas*, *Acc*, *Scd1*, and *Elovl6* in the liver was measured by qRT-PCR and normalized to 18S rRNA. **f** HepG2 cells were cultured for 24 h in the presence of PTE, treated with or without static (5 µM) for 1 h followed by IL-6 for 15 min or 8 h, and STAT3 phosphorylation, total STAT3, SREBP-1c, and β-actin were detected by western blotting. **g** HepG2 cells were cultured for 24 h in the presence of PTE and treated with or without static (5 µM) for 1 h, followed by IL-6 and OA treatment for 24 h, after which lipid droplets in the cells were assayed using ORO staining and intracellular TG was measured. The original magnification was ×200. All data are presented as the mean ± SD. **P* < 0.05, ***P* < 0.01, ****P* < 0.001

PTE improved hepatic inflammation and insulin resistance in HFD-fed mice

To address whether PTE influences pro-inflammatory gene expression, we assessed expression of *Tnfx*, *Mcp1*, *Il1β*, and *Il6* in the livers of mice fed the HFD or ND with or without PTE. PTE decreased *Tnfx*, *Mcp1*, and *Il1β*

expression in the livers of HFD-fed mice, whereas it failed to alter IL-6 expression in the livers of HFD-fed or ND-fed mice (Fig. 4a). PTE inhibited STAT3 phosphorylation induced by IL-6 in RAW264.7 macrophages and U937 cells (Fig. 4b), suggesting that PTE treatment conserved almost intact ALT/AST levels in the liver of HFD-fed mice by inhibiting inflammatory responses (Fig. 1g, h).

However, it cannot be ruled out that PTE directly protected against lipotoxicity. To address this possibility we incubated HepG2 cells with the lipotoxic free fatty acid, palmitate PA [32] and examined whether PTE inhibited PA-induced cell death. We found that PTE did not prevent the lipotoxicity of PA (Supplementary Fig. 3). Collectively, these results suggested that the protective effects of PTE on inflammatory liver responses might at least partly participate in the protection against liver damage in HFD-fed mice.

Insulin resistance is a hallmark of NAFLD. To assess key parameters of glucose homeostasis in HFD-fed mice, we performed IPITTs and IPGTTs. PTE significantly enhanced glucose tolerance and insulin

sensitivity in HFD-fed mice, but not in ND-fed mice (Fig. 4c, d). In addition, we examined molecules that regulate insulin signaling and gluconeogenesis-associated genes in the liver. Consistently, HFD-fed mice showed reduced mRNA levels of *Irs2*, a cytoplasmic signaling molecule required for insulin signaling, as well as increased mRNA levels of *Foxo1*, *Pck1*, and *G6pase*, in the liver (Fig. 4e). In contrast, PTE treatment clearly enhanced *Irs2* expression and significantly reduced expression of gluconeogenesis-associated genes (Fig. 4e). These results suggested that PTE prevented HFD-induced metabolic disorders through inhibition of hepatic inflammatory responses and maintenance of normal insulin signaling.

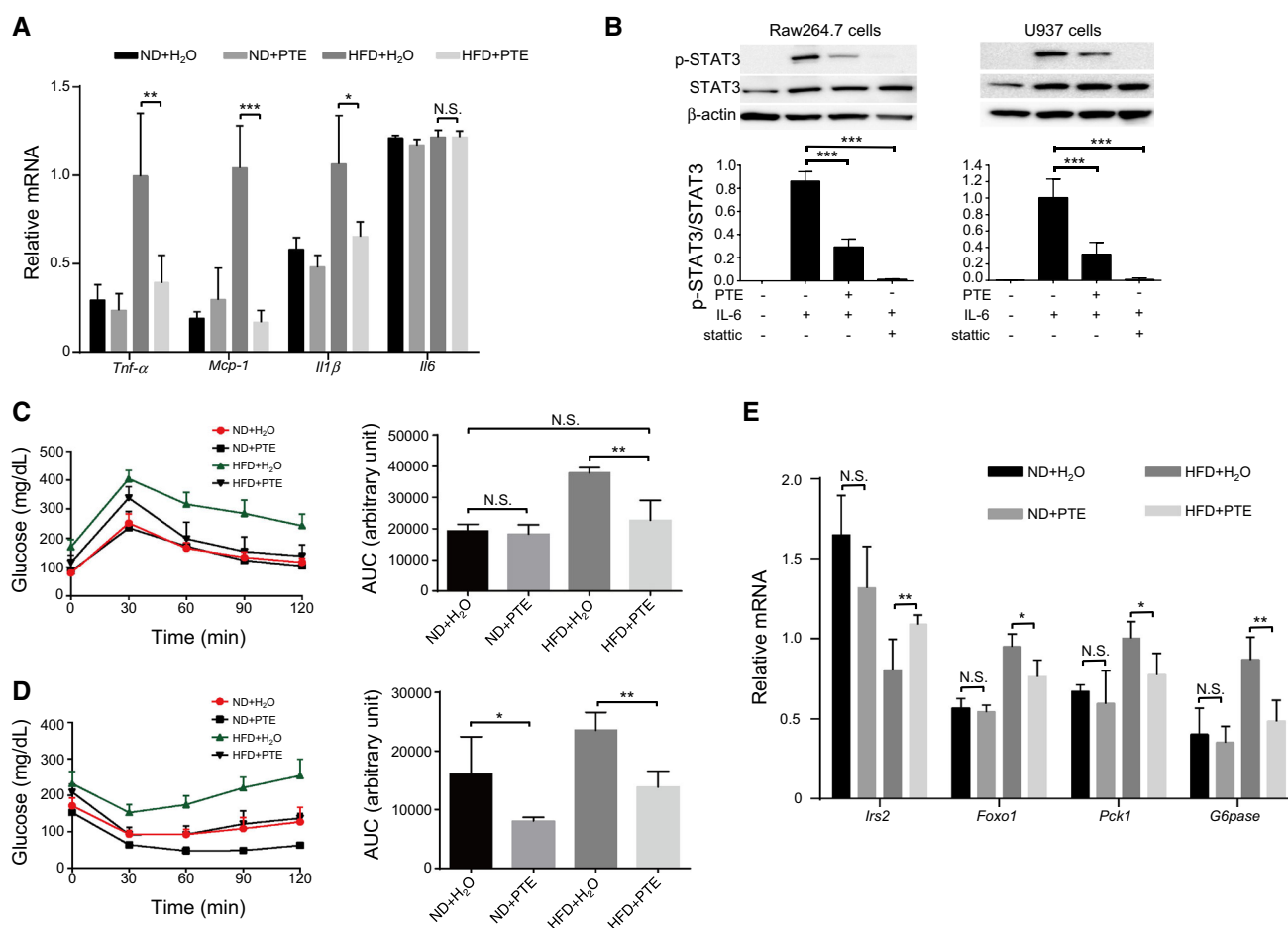


Fig. 4 PTE suppresses hepatic induction of pro-inflammatory cytokines and improves insulin resistance in HFD-fed mice. **a** Relative mRNA expression of pro-inflammatory cytokine genes such as *Tnfα*, *Mcp1*, *Il1β*, and *Il6* in the liver was measured by qRT-PCR. The amount of each mRNA transcript was normalized to the level of *18S* rRNA. **b** RAW264.7 cells and U937 cells were treated with PTE for 1 h, followed by IL-6 (2 ng/mL) for 15 min, and STAT3 phosphorylation, total STAT3 expression, and β-actin expression were detected by western blotting. The p-STAT3/STAT3 ratio was

quantified and statistical analysis was performed. IPGTTs (c) and IPITTs (d) were performed on ND- and HFD-fed mice at week 17 and the area under the curve was calculated. **e** Relative mRNA expression of gluconeogenesis-associated genes such as *Irs2*, *Foxo1*, *Pck1*, and *G6pase* in the liver was measured by qRT-PCR. The amount of each mRNA transcript was normalized to the level of *18S* rRNA. All data are the mean ± SD for five mice/group. * $P < 0.05$, ** $P < 0.01$, *** $P < 0.001$

Discussion

Pu-erh tea, a fermented dark tea originating in China, is widely consumed in southeastern Asia owing to its unique flavor and potential health benefits. In the present study, we showed that PTE enhanced IL-6/STAT3 signaling in hepatocytes, downregulated expression of lipogenesis- and gluconeogenesis-associated genes in the liver, and protected against hepatic steatosis in HFD-fed mice. In hepatocytes, PTE potently upregulated *PPAR α* , a master regulator of lipid β -oxidation [33]. We also showed that PTE improved insulin resistance and downregulated expression of pro-inflammatory cytokines in the liver. The effects of PTE on gene expression might be responsible for its inhibitory effect on the development of NASH in HFD-fed mice.

Our results indicate that PTE enhances hepatocytic IL-6/STAT3 signaling in vivo and in vitro, suggesting that the activation of hepatocytic STAT3 has a role in the prevention of HFD-induced steatohepatitis and improvement of insulin resistance by PTE. STAT3 is a transcription factor that mediates the expression of a variety of genes upon stimulation with diverse stimuli; thus, STAT3 plays a key role in many cellular processes such as inflammation and cell growth. IL-6 can activate STAT3 through binding to the IL-6 receptor and gp130, a transmembrane protein important for signal transduction. Because IL-6 is assumed to act as a pro-inflammatory cytokine, our results may seem unexpected. In fact, it has been proposed that IL-6 contributes to the progression of many inflammatory diseases such as rheumatoid arthritis and Crohn's disease [34, 35]. However, the role of IL-6 signaling in NASH remains highly controversial. Hepatic and circulating levels of IL-6 are elevated in patients with NASH [36, 37]. Nonetheless, it has been clearly verified that IL-6 and its signaling in hepatocytes contribute to the amelioration of hepatic steatosis in HFD-fed mice. Hepatocyte-specific gp130-deficient mice are predisposed to hepatic steatosis, while IL-6 treatment and hepatic introduction of a constitutively active form of STAT3 prevent leptin- and leptin receptor-deficient obese mice from developing hepatic steatosis [15, 25, 26]. Mice fed ad libitum with HFD are characterized by increased lipogenesis and decreased fatty acid oxidation in the liver, resulting in gradual accumulation of lipid droplets in the hepatocytes [38]. The anti-steatogenic effect of STAT3 in hepatocytes is mediated, at least in part, via inhibition of SREBP-1c, a master regulator that controls lipid biosynthesis, and subsequent suppression of hepatic lipogenesis [25, 39]. In fact, it has been demonstrated that STAT3 mediates inhibition of SREBP-1c promoter activity [40]. It is intriguing that treatment with PTE downregulated induction of SREBP-1c and its downstream lipogenic

enzymes Fas, Acc, Scd1, and Elovl6, concomitant with elevation of STAT3 phosphorylation, in the livers of HFD-fed mice. These results imply that PTE treatment protects against HFD-induced NASH at least partially via enhancement of STAT3 signaling together with endogenous IL-6/STAT3 signaling in liver parenchymal cells.

There is general agreement that mild portal endotoxemia can be detected in healthy subjects because of translocation of gut-derived bacterial lipopolysaccharide (LPS), also known as endotoxin [41, 42]. When exposed to LPS, the liver produces low levels of IL-6 [27, 28]. Therefore, we treated HepG2 cells with PTE in the presence of IL-6. In HepG2 cells, PTE enhanced IL-6/STAT3 signaling, decreased SREBP-1c protein expression, and inhibited lipid droplet accumulation. Furthermore, the STAT3 phosphorylation inhibitor stat3c abolished the protective action of IL-6/PTE, resulting in normal accumulation of lipid droplets. We also found that PTE treatment significantly increased the expression of *PPAR α* in HepG2 cells. Intriguingly, in sharp contrast with PTE, IL-6 failed to induce *PPAR α* gene expression in HepG2 cells, suggesting that increased fatty acid β -oxidation in hepatocytes due to PTE was likely mediated by STAT3-independent mechanisms. Our data indicate that PTE inhibited lipogenesis by enhancing IL-6/STAT3 signaling, while PTE increased fatty acid oxidation via IL-6-independent signaling.

It has been recently reported that PTE suppresses fatty acid synthase via activating AMPK and via downregulating Akt and JNK signaling. However, we did not observe such effects of PTE in this study (Supplementary Fig. 2). This might be due to differences in the sources of PTE.

In contrast to hepatocytes, PTE downregulated IL-6/STAT3 signaling in macrophages. These distinct effects might be due to differential actions of PTE on between HepG2 cells and macrophages. For example, PTE might induce potent, endogenous inhibitor of the IL-6 signaling, such as suppressor of cytokine signaling (SOCS)1 and/or SOCS3, in macrophages but not in hepatocytes. Further, PTE might upregulate expression of IL-6R consisting of IL-6R α and gp130 in hepatocytes, but not in macrophages. Further study is needed to clarify the mechanism by which PTE affects the IL-6/STAT3 pathway oppositely in those two types of cells.

Importantly, in vivo treatment with PTE reduced hepatic inflammation concomitantly with reduced induction of *Tnf α* , *Mcp1*, and *Il1 β* in the livers of HFD-fed mice. Inflammation is an important contributing factor to NASH pathogenesis [43]. Therefore, protection against hepatic inflammatory responses by PTE might partially account for the poor development of NAFLD/NASH in the PTE-treated animals. However, further study is required to determine whether, and how, reduced STAT3 signaling in

macrophages is associated with the poor inflammatory responses observed in the livers of PTE-treated, HFD-fed mice.

Insulin resistance, a hallmark of NAFLD, is often associated with impaired insulin signaling due to either decreased insulin concentrations or functional modifications of crucial signaling molecules, including IRS. Down-regulation of PCK-1 and G6Pase, key enzymes involved in gluconeogenesis, is dependent on hepatic IL-6/STAT3 signaling [25, 44]. IRS-2 is abundantly expressed in the liver and is mainly associated with the inhibition of PCK-1 and G6Pase expression [45]. Although treatment with PTE did not affect *Ilf6* expression levels in vivo, it enhanced STAT3 phosphorylation and *Irs2* expression, while significantly reducing the induction of *Pck1*, *G6pase*, and *Foxo1* in the livers of HFD-fed mice, suggesting that PTE may repress gluconeogenesis via STAT3 signaling, but not by inducing IL-6. Taken together, these data provide strong evidence that PTE ameliorates HFD-induced NASH and insulin resistance by modulating hepatic IL-6/STAT3 signaling. However, the mechanism by which PTE modulates IL-6/STAT3 signaling is unclear. Further studies, for example, using hepatocyte-specific STAT3 knockout mice, are required to verify the crucial role of IL-6/STAT3 signaling in PTE-associated prevention of steatohepatitis.

In this study, we determined that PTE attenuates NASH and insulin resistance in a manner dependent on IL-6/STAT3 signaling in the liver, suggesting that PTE could be used as a means of preventing and treating NASH.

Acknowledgments We thank Mss. Nana Iwami, Keiko Mitani, and Tomoko Mizobuchi for their excellent technical assistance. We also thank Drs. Hiroko Iijima and Koubun Yasuda for helpful discussions. Xianbin Cai was supported by the State Scholarship Fund of China Scholarship Council (CSC). This study was partly supported by the MEXT-Supported Program for the Strategic Research Foundation at Private Universities, 2012–2015 and by the Pu'erh Tea Research Institute (Yunnan, China).

Compliance with ethical standards

Conflict of interest The authors declare that they have no conflict of interest.

References

- Clark JM, Brancati FL, Diehl AM. The prevalence and etiology of elevated aminotransferase levels in the United States. *Am J Gastroenterol*. 2003;98:960–7.
- Adams LA, Lymp JF, Sauver JS, et al. The natural history of nonalcoholic fatty liver disease: a population-based cohort study. *Gastroenterology*. 2005;129:113–21.
- Lazo M, Hernaez R, Eberhardt MS, et al. Prevalence of nonalcoholic fatty liver disease in the United States: the third national health and nutrition examination survey, 1988–1994. *Am J Epidemiol*. 2013;178:38–45.
- Kim D, Choi S-Y, Ha Park E, et al. Nonalcoholic fatty liver disease is associated with coronary artery calcification. *Hepatology*. 2012;56:605–13.
- Tokushige K, Hashimoto E, Horie Y, et al. Hepatocellular carcinoma in Japanese patients with nonalcoholic fatty liver disease, alcoholic liver disease, and chronic liver disease of unknown etiology: report of the nationwide survey. *J Gastroenterol*. 2011;46:1230–7.
- Fan J-G. Epidemiology of alcoholic and nonalcoholic fatty liver disease in China. *J Gastroenterol Hepatol*. 2013;28(Suppl 1):11–7.
- Weiß J, Rau M, Geier A. Non-alcoholic fatty liver disease: epidemiology, clinical course, investigation, and treatment. *Dtsch Arztebl Int*. 2014;111:447–52.
- Day CP, James OFW. Steatohepatitis: a tale of two “hits”? *Gastroenterology*. 1998;114:842–5.
- Farrell GC, van Rooyen D, Gan L, et al. NASH is an inflammatory disorder: pathogenic, prognostic and therapeutic implications. *Gut Liver*. 2012;6:149–71.
- Wang C-Y, Liao JK. A mouse model of diet-induced obesity and insulin resistance. *Methods Mol Biol*. 2012;821:421–33.
- Lee LK, Foo KY. Recent advances on the beneficial use and health implications of Pu-erh tea. *Food Res Int*. 2013;53:619–28.
- Kubota K, Sumi S, Tojo H, et al. Improvements of mean body mass index and body weight in preobese and overweight Japanese adults with black Chinese tea (Pu-Erh) water extract. *Nutr Res*. 2011;31:421–8.
- Yan S-J, Wang L, Li Z, et al. Inhibition of advanced glycation end product formation by Pu-erh tea ameliorates progression of experimental diabetic nephropathy. *J Agric Food Chem*. 2012;60:4102–10.
- Du W-H, Liu Z, Shi L, et al. Hypoglycemic effect of the water extract of Pu-erh tea. *J Agric Food Chem*. 2012;60:10126–32.
- Kroy DC, Beraza N, Tschahardaneh DF, et al. Lack of interleukin-6/glycoprotein 130/signal transducers and activators of transcription-3 signaling in hepatocytes predisposes to liver steatosis and injury in mice. *Hepatology*. 2010;51:463–73.
- Yu Y, Hayashi S, Cai X, et al. Pu-erh tea extract induces the degradation of FET family proteins involved in the pathogenesis of amyotrophic lateral sclerosis. *Biomed Res Int*. 2014;. doi:10.1155/2014/254680.
- Schust J, Speri B, Holis A, et al. Stattic: a small-molecule inhibitor of STAT3 activation and dimerization. *Chem Biol*. 2006;13:1235–42.
- Vidyashankar S, Varma RS, Patki PS. Quercetin ameliorates insulin resistance and up-regulates cellular antioxidants during oleic acid induced hepatic steatosis in HepG2 cells. *Toxicol Vitro*. 2013;27:945–53.
- Luo X, Yang Y, Shen T, et al. Docosahexaenoic acid ameliorates palmitate-induced lipid accumulation and inflammation through repressing NLRC4 inflammasome activation in HepG2 cells. *Nutr Met*. 2012;. doi:10.1186/1743-7075-9-34.
- Folch J, Lees M, Sloane Stanley GH. A simple method for the isolation and purification of total lipids from animal tissues. *J Biol Chem*. 1957;226:497–509.
- Kleiner DE, Brunt EM, Van Natta M, et al. Design and validation of a histological scoring system for nonalcoholic fatty liver disease. *Hepatology*. 2005;41:1313–21.
- Schneider CA, Rasband WS, Eliceiri KW. NIH Image to ImageJ: 25 years of image analysis. *Nat Methods*. 2012;9:671–5.
- Kato J, Okamoto T, Motoyama H, et al. Interferon-gamma-mediated tissue factor expression contributes to T-cell-mediated

- hepatitis through induction of hypercoagulation in mice. *Hepatology*. 2013;57:362–72.
24. Liu Q, Rehman H, Krishnasamy Y, et al. Role of inducible nitric oxide synthase in mitochondrial depolarization and graft injury after transplantation of fatty livers. *Free Radic Biol Med*. 2012;53:250–9.
 25. Inoue H, Ogawa W, Ozaki M, et al. Role of STAT-3 in regulation of hepatic gluconeogenic genes and carbohydrate metabolism *in vivo*. *Nat Med*. 2004;10:168–74.
 26. Hong F, Radaeva S, Pan H-N, et al. Interleukin-6 alleviates hepatic steatosis and ischemia/reperfusion injury in mice with fatty liver disease. *Hepatology*. 2004;40:933–41.
 27. Jacob AI, Goldberg PK, Bloom N, et al. Endotoxin and bacteria in portal blood. *Gastroenterology*. 1977;72:1268–70.
 28. Diehl AM. Cytokine regulation of liver injury and repair. *Immunol Rev*. 2000;174:160–71.
 29. Barclay JL, Nelson CN, Ishikawa M, Murray LA, Kerr LM, McPhee TR, Powell EE, Waters MJ. GH-dependent STAT5 signaling plays an important role in hepatic lipid metabolism. *Endocrinology*. 2011;152:181–92.
 30. Huang HC, Lin JK. Pu-erh tea, green tea, and black tea suppresses hyperlipidemia, hyperleptinemia and fatty acid synthase through activating AMPK in rats fed a high-fructose diet. *Food Funct*. 2012;3:170–7.
 31. Chiang CT, Weng MS, Lin-Shiau SY, Kuo KL, Tsai YJ, Lin JK. Pu-erh tea supplementation suppresses fatty acid synthase expression in the rat liver through downregulating Akt and JNK signalings as demonstrated in human hepatoma HepG2 cells. *Oncol Res*. 2005;16:119–28.
 32. Noguchi Y, Young JD, Aleman JO, Hansen ME, Kelleher JK, Stephanopoulos G. Effect of anaplerotic fluxes and amino acid availability on hepatic lipoapoptosis. *J Biol Chem*. 2009;284:33425–36.
 33. Pawlack M, Lefebvre P, Staels B. Molecular mechanism of PPARalpha action and its impact on lipid metabolism, inflammation and fibrosis in non-alcoholic fatty liver disease. *J Hepatol*. 2015;62:720–33.
 34. Ishihara K, Hirano T. IL-6 in autoimmune disease and chronic inflammatory proliferative disease. *Cytokine Growth Factor Rev*. 2002;13:357–68.
 35. Atreya R, Mudter J, Finotto S, et al. Blockade of interleukin 6 trans signaling suppresses T-cell resistance against apoptosis in chronic intestinal inflammation: evidence in Crohn disease and experimental colitis *in vivo*. *Nat Med*. 2000;6:583–8.
 36. Tarantino G, Conca P, Pasanishi F, et al. Could inflammatory markers help diagnose nonalcoholic steatohepatitis? *Eur J Gastroenterol Hepatol*. 2009;21:504–11.
 37. Wieckowska A, Papouchado BG, Li ZZ, et al. Increased hepatic and circulating interleukin-6 levels in human nonalcoholic steatohepatitis. *Am J Gastroenterol*. 2008;103:1372–9.
 38. Chaix A, Zarrinpar A, Miu P, Panda S. Time-restricted feeding is a preventative and therapeutic intervention against diverse nutritional challenges. *Cell Met*. 2014;20:991–1005.
 39. Wang H, Lafdil F, Kong X, Gao B. Signal transducer and activator of transcription 3 in liver diseases: a novel therapeutic target. *Int J Biol Sci*. 2011;7:536–50.
 40. Ueki K, Kondo T, Tseng YH, et al. Central role of suppressors of cytokine signaling proteins in hepatic steatosis, insulin resistance, and the metabolic syndrome in the mouse. *Proc Natl Acad Sci USA*. 2004;101:10422–7.
 41. Miele L, Valenza V, La Torre G, et al. Increased intestinal permeability and tight junction alterations in nonalcoholic fatty liver disease. *Hepatology*. 2009;49:1877–87.
 42. Triger DR, Boyer TD, Levin J. Portal and systemic bacteraemia and endotoxaemia in liver disease. *Gut*. 1978;19:935–9.
 43. Wellen KE, Hotamisligil GS. Inflammation, stress, and diabetes. *J Clin Invest*. 2005;115:1111–9.
 44. Awazawa M, Ueki K, Inaba K, et al. Adiponectin enhances insulin sensitivity by increasing hepatic IRS-2 expression via a macrophage-driven IL-6-dependent pathway. *Cell Met*. 2011;13:401–12.
 45. Kubota N, Kubota T, Itoh S, et al. Dynamic functional relay between insulin receptor substrate 1 and 2 in hepatic insulin signaling during fasting and feeding. *Cell Met*. 2008;8:49–64.